Environmental Science
Processes & Impacts

Accepted Manuscript

ROYAL SOCIETY OF CHEMISTRY

rsc.li/process-impacts

Environmental Impact

Iron (oxy)hydroxides is of important component of soil that controlled the most radionuclides behaviors in environment. The mobility of U(VI) in environmental medium is mainly controlled by its adsorption mechanism that is affected by the characteristics of the host phase, pH, the speciation of U(VI) in aqueous phase, ionic strengthen, organic matters, and temperature. This study mainly discussed the influence of the surface properties of iron (oxy)hydroxides, organic matters, temperature, pH on U(VI) sorption and the sorption species of U(VI) by the surface complexation model. These findings are crucial to evaluate the immobilization of U(VI) in the surrounding of the uranium mill tailing ponds, deep geological repositories of high level radioactive wastes, spent fuel storage facilities and also important to the environmental protection and remediation.

Immobilization of U(VI) on iron oxy-hydroxides under various physicochemical conditions

Ping LI[a], Zhuoxin YIN[a], Jianfeng LIN[b], Qiang JIN[a], Yaofang DU[a], Qiaohui FAN[a*], Wangsuo WU[a*]

[a] Radiochemistry Laboratory, School of Nuclear Science and Technology, Lanzhou University, Lanzhou, Gansu 730000 China;

[b] Northwest Institute of Nuclear Technology, Xi'an, Shanxi, 710024 China

Abstract: The immobilization of U(VI) at solid/water interface is an important process related to its transportation and migration in environment, which is dominantly controlled by its sorption behavior of U(VI). In this study, U(VI) sorption on Fe(II) and Fe(III) oxy-hydroxides prepared using co-precipitation method was studied at various physicochemical conditions such as pH, ionic strength, humic acid (HA), and temperature. The results showed that the sorption of U(VI) on iron oxy-hydroxides is chemical sorption and that intra-particle diffusion is main rate limitation. The sorption of U(VI) on iron oxy-hydroxides was strongly dependent on pH but weakly on ionic strength in the whole observed pH range.

At acidic condition, the presence of HA can enhance U(VI) sorption to a large extent, a inhibition effect on the sorption of U(VI), however, can be observed under alkaline condition with respect to soluble U(VI)-HA complexes. The sorption U(VI) on iron oxy-hydroxides is an endothermic process and is in favor of high temperature. Surface complexation model suggested three dominant mono-dentate inner-sphere complexes of $\equiv S^{s}OUO_2^{+}$ (log$K$ = 1.65), $\equiv S^{w}OUO_2OH^{0}$ (log$K$ = -8.00), and $\equiv S^{w}OUO_2(CO_3)_2^{3-}$ (log$K$ = 17.50) contributing to U(VI) sorption on iron oxy-hydroxides over the observed pH range.

Keywords: U(VI), Iron oxy-hydroxides, Surface complexation model, Sorption, HA, Temperature

* Corresponding author. fanqiaohui@gmail.com (FAN Q.H.), wuws@lzu.edu.cn (WU W.S.)
Tel: +86-931-8913278; Fax: +86-931-8913594.

1. Introduction:

Uranium (U), as one of main radionuclides in nuclear industry is a key contaminant, due to its release from the concentrated regions, such as, uranium mill tailing ponds, deep geological repositories of high level radioactive wastes, and spent fuel storage facilities. As is well known, uranium occurs as a mobile aqueous UO_2^{2+} under natural condition, therefore the immobilization of UO_2^{2+} at solid/water interface related to its transportation becomes of great importance to environmental remediation and protection, which is mainly controlled by sorption and desorption of U(VI) at the solid/water interface.[1] The sorption of U(VI) on a multiplicity of naturally occurring and artificial substrates has been widely estimated in the last several decades using batch and column approaches, spectroscopic and microscopic analyses, theoretical calculations, and modeling.[2] There is a consensus that the sorption of U(VI) on minerals is a maximum at near neutral pH and sharply decreases towards more acidic or more alkaline conditions in air condition with the partial pressure of CO_2 about ~37.5 Pa.[3-6]

In many spent fuel disposal concepts, the vitrified waste package (vitrified waste + stainless steel container) for long-life and high radioactive isotopes will be overpacked in a non-alloy steel surcontainer.[7] In case of an infiltration of water, the first barrier to the migration of uranium would thus be the (corroded) surcontainer. Iron hydroxides, especially magnetite (Fe_3O_4) have been confirmed to be the main component of the corrosion products of steel surcontainer. It is why large amounts of researches have focused on the sorption of radionuclides on iron oxides.[8] The association of U with the amorphous and crystalline forms of iron oxides commonly formed on corroding steel surfaces.[9] Extended X-ray absorption fine structure (EXAFS) has confirmed uranyl oxy-hydroxides on the surfaces of goethite, maghemite, and magnetite, whereas bidentate inner-sphere complexes on ferrihydrite and lepidocrocite at molecular scale. Moreover, green rust can be converted to magnetite with concomitant reduction of U(VI) to U(IV).[9] Aamrani et al.[10] found that the sorption of U(VI) on magnetite has characteristics of both UO_2 and schoepite, and

that the sorption species on magnetite were actually a mixture of U(VI) and U(IV) as well. When Rovira et al.[11] further investigated the influence of the steel corrosion products on U released from the fuel, they found that the corroded steel was capable to not only adsorb U(VI), but also to reduce U(VI) to U(IV) at a high extent. It provides an effective retardation path to the migration of U out of repository. U(VI) sorption on magnetite can at least refer into three-stages: (i) the initial sorption of U(VI), (ii) possible reduction of U(VI) to UO_2 surface precipitation at surface-specific sites after 2−3 h of exposure, and (iii) the completion of U(VI) reduction after 6−8 h.[12]

The objectives of this study were to identify the immobilization of U(VI) on the synthesized Fe(III) and/or Fe(II) oxy-hydroxides under various physicochemical conditions. Moreover, the surface complexation model (SCM) was used to discuss the sorption species and mechanism of U(VI) on iron oxy-hydroxides as well.

2. Experimental

2.1 Chemicals

All chemicals used in the experiments were purchased as analytical purity without any further purification. Uranyl stock solution was prepared by dissolving uranyl nitrate hexahydrate ($UO_2(NO_3)_2 \cdot 6H_2O$) in Milli-Q water. The stock solution was kept at pH 3.0 and further used in the following sorption experiments. HA was extracted from Lintan County (Gansu province, China) soil and has been characterized in our previous work.[13]

Iron oxy-hydroxides samples were synthesized strictly following the recipe of our previous work.[14] The specific surface area of the prepared samples was measured using N_2-BET to be about 106 m^2/g. Mineral composition and the topography of the iron oxy-hydroxides were, respectively, analyzed by X-ray diffraction and SEM patterns. The results suggested that the synthetic iron oxy-hydroxides mainly consist of magnetite and the average particle size is less than100 nm.[14]

86

87 **2.2 Potentiometric titrations**

88 The acid-base surface chemistry of the iron oxy-hydroxides was determined by
89 potentiometric titration, which was conducted in a 100 mL Teflon vessel with a
90 polyethylene lid. The vessel was surrounded with a glass jacket to maintain a
91 temperature of 25 ± 1°C. A Teflon bar was used for stirring. All titrations were
92 conducted using a computer controlled PC-titration system (809 Titrando, Metrohm)
93 with a combination pH electrode (Metrohm 6.02). Argon was bubbled successively
94 through NaOH, $HClO_4$, and distilled water to exclude CO_2 (g). Before beginning the
95 titrations, iron oxy-hydroxides (5.0 g/L) and background electrolyte (0.01 mol/L
96 $NaClO_4$) were added to the vessel and purged with argon for at least 2 h. The pH was
97 quickly lowered to approximately 3.0 by addition of 1.4721 mol/L $HClO_4$ solution.
98 After 1 h of equilibrium, the suspensions were slowly back-titrated at a variable
99 increment (0.008 up to 0.15 mL, which was automatically adjusted to keep a stable
100 pH change value) with 0.0509 mol/L NaOH solution to pH 9.0. Each step was
101 allowed to stabilize until the pH drift was less than 0.005 pH unit per minute.

102

103 **2.3 Sorption procedure**

104 Kinetic sorption was conducted over a contact time range of 0–30 h in 10 mL
105 polyethylene tubes containing a 0.3 g/L suspension of iron oxy-hydroxides and a 0.01
106 mol/L $NaClO_4$ solution. After the above suspensions were shaken for 2 days, 0.6 mL
107 of 2.0×10^{-4} mol/L U(VI) stock solution was added. Deionized water was added to
108 maintain a total volume of 6.0 mL, and the pH of the sorption system was adjusted to
109 4.50 with negligible volumes of 0.01 or 0.1 mol/L $HClO_4$ or NaOH solutions. At the
110 desired contact time, the suspensions were separated by centrifugation at constant
111 temperature under 12, 000 rpm for 30 min. An aliquot of the supernatant solution (3.0
112 mL) was removed and the concentration of U(VI) was analyzed by spectrophotometry
113 at 650 nm by using UO_2^{2+}-Arsenazo III complexes.

Sorption isotherms at different temperatures were conducted over a U(VI) concentration range of 2.8×10^{-6} to 1.7×10^{-4} mol/L by preparing 10 mL polyethylene tubes containing 0.6 g/L suspensions of the sorbents and 0.01 mol/L $NaClO_4$ solution at pH ~4.50. After the mixed suspensions were shaken for 2 days, various volumes of U(VI) stock solution were added to achieve the desired U(VI) concentration. Deionized water was then added to maintain a total volume of 6.0 mL, and the pH was adjusted to 4.50 with negligible volumes of 0.01 or 0.1 mol/L $HClO_4$ or NaOH solutions. The subsequent steps were the same as the kinetic process.

The sorption edge was conducted over a pH range of 3.0–9.0 in a mixture suspension of 0.3 g/L iron oxy-hydroxides and a 0.001, 0.01 or 0.1 mol/L $NaClO_4$ solution. After shaking 2 days, 0.6 mL 2.0×10^{-4} mol/L U(VI) stock solution was added, and the subsequent steps were the same as kinetic investigation section.

All the experimental data were the average of the duplicate or triplicate experiments; the relative errors of the data were less than 5%. The concentration of U(VI) sorbed on iron oxy-hydroxides (q (mol·g^{-1})) was calculated from initial U(VI) concentration (C_0 (mol·L^{-1})) and final concentration in solution after equilibrium (C_e (mol·L^{-1})), the volume of the solution (V (ml)) and the mass of iron oxy-hydroxides (m (g)) with the equation: $q = (C_0\text{-}C_e)\times V/m$.

3. Results and discussion

3.1 Sorption sites of iron oxy-hydroxides

As is well known, the added OH^- in the titration process reacts in two ways: (i) reacts with the solid surface, and (ii) changes the pH values of suspension. However, the added OH^- only changes the solution pH values in blank system.[15,16] As can be seen from Fig. 1A that, iron oxy-hydroxides own high buffer ability to OH^- compared with the blank, because much larger volume of OH^- solution was consumed by the iron oxy-hydroxides suspension in comparison with blank system. Fig. 1B and C show the Gran plots of the back-titration data of blank and iron oxy-hydroxides. The

Gran function (G) can be calculated as follows[16]:

Acidic side: $G_a = (V_0 + V_{at} + V_b) \times 10^{-pH} \times 100$ (1)

Alkaline side: $G_b = (V_0 + V_{at} + V_b) \times 10^{-(13.8-pH)} \times 100$ (2)

where V_0 represents the initial volume of the suspension. V_{at} and V_b are the total volumes of acid solution and of OH^- added at each titration point, respectively. The hydroxyl ions added to the suspension are consumed by the following steps reflected in the Gran plots: neutralization of excess H^+ in the suspension (before V_{eb1}), reactions with the various receivers on iron oxy-hydroxides surfaces (between V_{eb1} and V_{eb2}), and only adjustment of the system pH (after V_{eb2}).[16] In short, V_{eb1} and V_{eb2}, respectively, represent for the start and end points of acid-base reaction on oxy-hydroxides surface. Therefore, the total concentration of consumed proton (*TOTH)* is the total concentration of consumed protons in the titration process, which can be calculated from the following equation (3)[17]:

$$TOTH = \frac{-(V_b - V_{eb1}) \times C_b}{V_0 + V_b} \quad (3)$$

where C_b and V_0 are the concentration of NaOH and the initial volume of suspension, respectively.

In this study, both "strong" site ($\equiv Fe^sOH$) and "weak" site ($\equiv Fe^wOH$) that can be either protonated or deprotonated were assumed to simulate the titration process. These processes can be described by the following equations:

$$\equiv Fe^sOH + H^+_{(s)} \leftrightarrow \equiv Fe^sOH_2^+ \qquad K^{int}_{Fe^sOH_2^+} \quad (4)$$

$$\equiv Fe^sOH \leftrightarrow \equiv Fe^sO^- + H^+_{(s)} \qquad K^{int}_{Fe^sO^-} \quad (5)$$

$$\equiv Fe^wOH + H^+_{(s)} \leftrightarrow \equiv Fe^wOH_2^+ \qquad K^{int}_{Fe^wOH_2^+} \quad (6)$$

$$\equiv Fe^wOH \leftrightarrow \equiv Fe^wO^- + H^+_{(s)} \qquad K^{int}_{Fe^wO^-} \quad (7)$$

where $\equiv Fe^sOH_2^+$ ($\equiv Fe^wOH_2^+$), $\equiv Fe^sOH$ ($\equiv Fe^wOH$) and $\equiv Fe^sO^-$ ($\equiv Fe^wO^-$), represent protonated, neutral, and deprotonated surface hydroxyl function groups, respectively. $H^+_{(s)}$ is the proton concentration on the surface of iron oxy-hydroxides. $K^{int}_{Fe^sOH_2^+}$ and

168 $K^{int}_{Fe^wOH_2^+}$ are intrinsic acidity constants of the protonation process, and $K^{int}_{Fe^sO^-}$ and
169 $K^{int}_{Fe^wO^-}$ are intrinsic acidity constants of the deprotonation process.

170 The titration data can be simulated well basing on the above assumptions
171 combined the MINTEQ 3.0 code (Fig. 1D). The results suggested that the two-site
172 model and a constant capacity model (CCM) are efficient to the titration of iron
173 oxy-hydroxides. The distribution of each site as a function of pH is shown in Fig. 2
174 and the relative parameters are summarized in Table 1. Both $\equiv Fe^wOH$ and $\equiv Fe^sOH$
175 are the main sorption sites for iron oxy-hydroxides. The concentrations of $\equiv Fe^wOH_2^+$,
176 $\equiv Fe^sOH$ and $\equiv Fe^sOH_2^+$ decrease with a increase in pH, while the species of $\equiv Fe^wO^-$
177 and $\equiv Fe^sO^-$ gradually prevail. The concentration distribution of $\equiv Fe^wOH$ is in
178 agreement with the protonation and deprotonation reactions (6)–(7). As discussed
179 above, the distribution of sorption sites is strong pH-dependence, indicating that the
180 sorption of U(VI) on the iron oxy-hydroxides should be strongly dependent on
181 solution pH and that the inner-sphere complexes will be the main sorption species.

182

183 **3.2 Kinetic estimation on U(VI) sorption**

184 Fig. 3A shows that the sorption of U(VI) on the iron oxy-hydroxides achieves
185 equilibrium within 10 hours; thereby 2 days were chosen for the subsequent
186 experiments to ensure the equilibrium of U(VI) sorption. Knowledge of the kinetics
187 can be important not only for modeling the migration of radionuclides but also for the
188 elucidation of their sorption mechanism. In this study, three kinds of models were
189 employed to study the kinetic process of U(VI) sorption on the iron oxy-hydroxides,
190 and the equations of each model and the results of linear simulations were
191 summarized in Fig. 3 and Table 2. One can see that the calculated correlation
192 coefficients are much closer to unity (R^2=0.9993) for the pseudo-second-order kinetics
193 model in comparison with the pseudo-first-order kinetic model (R^2=0.8369). This
194 result suggested that the sorption process of U(VI) on the iron oxy-hydroxides can be

described well using the pseudo-second-order model for U(VI) sorption, where the sorption of U(VI) will, as expected, be affected by both the amount of adsorbent and the concentration of U(VI). In addition, the pseudo-second-order model assumes that the controlling step should be attributed to chemical sorption.[20]

For the intra-particle diffusion model, generally, if the adsorption steps are independent of one another, the plot of q_t versus $t^{1/2}$ usually shows two or more intercepting lines depending upon the exact mechanism.[21] The present multi-linearity indicates that U(VI) sorption on the iron oxy-hydroxides actually experiences at least three steps as shown in Fig. 3B. The first faster step is attributed to the diffusion of U(VI) ions through the bulk of solution to the external surface of iron oxy-hydroxides and/or the boundary layer diffusion of solute molecules. The second step describes the gradual sorption stage, where intra-particle diffusion is rate limitation for the sorption of U(VI). The third step can be attributed to the final equilibrium stage. Values of the intra-particle diffusion constants (K_{int1}, K_{int2} and K_{int3}) and the correlation coefficients (R) for the three steps are listed in Table 2. The results demonstrate that the sorption of U(VI) on the iron oxy-hydroxides may be followed by an intra-particle diffusion from ~0.8 to ~2.6 h. It indicates that the intra-particle diffusion was the main rate-controlling step.[22]

3.3 Effect of solid-to-liquid (*s/l*) ratio

The influence of solid-to-liquid ratio (*s/l*) on U(VI) sorption to iron oxy-hydroxides is shown in Fig. 4. As expected, higher *s/l* is desirable for U(VI) sorption in the range of 0.1~1.8 g/L. It can be interpreted by the fact that more sorption sites are available to U(VI) sorption with an increase in the content of iron oxy-hydroxides.[23,24] The *s/l*-dependence is actually consistent with the prediction of the pseudo-second-order model in the kinetic estimation as above. The distribution coefficient ($K_{d,}$ mL/g) as a function of *s/l* is also plotted in Fig. 4. K_d can be calculated from the concentration of U(VI) in suspension (C_0) and that of U(VI) in supernatant (C_e) according to the following equation:

$$K_d = \frac{C_0 - C_e}{C_e} \cdot \frac{V}{m} \qquad (8)$$

where V is the volume of the suspension (mL) and m is the mass of iron oxy-hydroxides (g). It is necessary to note that the value of K_d is weakly dependent on *s/l*, which is consistent with the physicochemical properties of K_d value, i.e., K_d is independent of the ratio of *s/l* at very low solid content. The results are consistent with Eu(III) sorption on alumina and Pb(II) on Na-rectorite.[15,25]

3.4 Effect of pH and ionic strength

U(VI) sorption to the iron oxy-hydroxides as a function of pH is investigated at different ion strengths (i.e., 0.001, 0.01, and 0.1 mol/L $NaClO_4$) (Fig. 5A). The sorption of U(VI) on the iron oxy-hydroxides increased sharply from ~0% (pH ~3.0) to ~96% (pH ~5.5). The increasing sorption of U(VI) can be attributed to the progressive deprotonation of the sorption site (≡*FeOH*) on iron oxy-hydroxides with a increase of pH to develop a negative charged surface. The electrostatic attraction, therefore, becomes increasingly large between the negative charged surface and the positive speciation of U(VI) (main UO_2^{2+}) in the pH range of 3.0-5.5.

Around the neutral conditions, several species ($UO_2(OH)^+$, $UO_2CO_3^0$ and $UO_2(CO_3)_2^{2-}$) are dominant for U(VI) in aqueous solution, simultaneously, the deprontonated sorption sites are increasingly developing as pH increases. These processes may be accompanied with the strong sorption, that is, inner-sphere complexes on the iron oxy-hydroxides surface and with the formation of aqueous polynuclear complexes that can be adsorbed on the surface or that can possibly cause a process of surface precipitation.[26-28] Müller et al.[29] confirmed that surface precipitation of U(VI) can form at the late sorption stage using both in-situ vibrational spectroscopy and EXAFS approaches.

As expected, the sorption of U(VI) on the iron oxy-hydroxides decreased above pH 7.5, because the soluble formation of negative charged U(VI)-carbonate complexes in solution (mainly $UO_2(CO_3)_3^{4-}$) and the negative charged surface become

prevailed at alkaline condition.[30]

The influence of ionic strength on U(VI) sorption on the iron oxy-hydroxides is shown in Fig. 5. One can see that U(VI) sorption is weakly dependent on ionic strength in the whole pH range (Fig. 5B), particularly in alkaline condition. In theory, the inner-sphere complexes suggested by the SCM should not be affected to a large extent in the sorption of U(VI) by various ionic strength in terms of their strong sorption affinity. By contrast, outer-sphere complexes are expected to be more susceptible to the variation of ionic-strength at low pH range.[31] As is well known, the inner-sphere complexes are forming in the double layer of surface that can be compressed in thickness and capacity to some extent by the high salinity. Therefore the high ionic strength can slightly reduce the sorption of U(VI) on the iron oxy-hydroxides as shown in Fig. 5B. The higher sorption of U(VI) found at large *s/l* possibly suggests that such compressed effect by ionic strength on U(VI) sorption can be weakened by increasing the ratio of *s/l* because more sorption sites are available at larger *s/l*.

3.5 Effect of HA

Humic substances are the major natural-occurring organic compounds in surface water and soils. It can influence the migration and the transportation of radionuclides in several ways and can perform a vital influence on their bioavailability, toxicity, and mobility in the environment.[32,33] The effects of HA on U(VI) sorption are graphically presented in Fig. 6. In the presence of HA, the sorption edge shifts to lower pH with an increase of HA concentration from 0 to 50 mg/L (Fig. 6A). At low pH, the increment of U(VI) sorption can be expected because HA molecules can easily cover the positively charged surfaces of iron oxy-hydroxides as a result of an increase electrostatic attraction between U(VI) and the hybrid of HA/iron oxy-hydroxides. The strong complexation ability of HA molecule with U(VI) thus results in the large enhancement of U(VI) sorption. By contrast, HA becomes favor to retain in aqueous phase to form the stable but soluble complexes of U-HA that can reduce the sorption

of U(VI) to large extent as pH increases.[14,31,32]

The influence of HA addition sequence on radionuclides sorption mechanism is always controversy, and yet the investigation on HA addition sequence is very important to eliminate the controversy. Fig. 6B shows no conspicuous difference at various addition sequence of HA, indicating that HA molecules adsorbed are identical to those remaining in solution. However, Gu et al.[34] stated that the sorption of metal ion on iron oxide was affected by the sequence of the addition of humic substances, because the speciation of HA adsorbed iron oxy-hydroxides surface is different from that retained in solution. As well, no visible discrepancies of Eu(III) sorption was observed at different sequences of HA addition for the ternary attapulite/HA/Eu(III) system; howbeit EXAFS analysis clearly confirmed that different local atomic environments of Eu(III) were formed at various sequences of HA addition. The finding shows the different sorption species and mechanism for radionuclides in complicated conditions, even though the apparent sorption behavior seems similar at macro scale.[35]

3.6 Effect of temperature and thermodynamic estimation

Sorption isotherms of U(VI) on the synthetic iron oxy-hydroxides at different temperatures (i.e., 298 K, 318 K and 338 K) have been shown in Fig. 7A. The sorption of U(VI) is strongly dependent on temperature, indicating that the sorption of U(VI) on the iron oxy-hydroxides is more favored to occur at higher temperature. Results of present study confirm that various sorbents have positive response to the increase in temperature with respect to metal ions (Cs(I), Pb(II), Eu(III), Th(IV)) sorption.[13,36-38] The increase of temperature is known to increase the rate of diffusion of sorbate across the external boundary layer and in the internal pores of sorbent particles.[39] It can be due to the acceleration of some originally slow sorption steps or due to the retardation of the processes such as association of ions, aggregation of molecules, ion pairing and complex formation in the system.[40,41] The second possible reason is that the hydrolysis of cations proceeds to a greater extent as temperature

increases. The increase in temperature will thus reduce the electrostatic repulsion between the surface and the sorbate, allowing sorption to occur more readily.[35,42]

In order to get a better understanding of the sorption mechanism of U(VI) on the iron oxy-hydroxides, both Langmuir and Freundlich models are adopted to describe experimental sorption isotherms of U(VI). The Langmuir model is widely used for modeling equilibrium data. It is valid for monolayer sorption on surface containing finite number of identical sites. The form of the Langmuir isotherm can be represented by the equation (9):

$$q = \frac{bq_{\max}C_e}{1+bC_e} \qquad (9)$$

where C_e is the equilibrium concentration of metal ions remained in the solution ($mol \cdot L^{-1}$); q is the amount of U(VI) sorbed on per weight unit of solid after equilibrium ($mol \cdot g^{-1}$); q_{max}, the maximum sorption capacity, is the amount of U(VI) at complete monolayer coverage ($mol \cdot g^{-1}$) and b is a constant that relates to the heat of sorption ($L \cdot mol^{-1}$). The Freundlich expression is an empirical equation describing sorption on a heterogeneous surface with infinite identical sites and is expressed by the following equation:

$$q = k_F C_e^{\,n} \qquad (10)$$

where k_F ($mol^{1-n} \cdot g^{-1} \cdot L^n$) represents the sorption capacity when U(VI) ion equilibrium concentration equals 1, and n represents the degree of dependence of sorption with equilibrium concentration. The related parameters have been listed in Table 3. The results suggest that the Langmuir isotherm provides a good model of the sorption system. This finding is in accordance with U(VI) sorption on hematite.[31] The fitting of sorption data to Langmuir isotherm reveals that the sorption occurs in a monolayer or the sorption may only occur at a fixed number of localized sites of iron oxy-hydroxides surface.

The thermodynamic parameters of U(VI) sorption can be calculated from the temperature-dependent sorption. The free energy changes (ΔG^0) are calculated by the following equation:

$$\Delta G^0 = -R \cdot T \cdot \ln K^0 = -2.3026 \cdot R \cdot T \cdot \log K^0 \quad (11)$$

where R is the ideal gas constant (8.314 $J \cdot mol^{-1} \cdot K^{-1}$), T is the temperature in Kelvin, and K^0 is the sorption equilibrium constant. The $\log K^0$ can be extrapolated from the plotting of $\log K_d$ vs. C_e when C_e is close to zero as shown in Fig. 7B.[43] The relative parameters of the linear fit of $\log K_d$ vs. C_e for U(VI) sorption on iron oxy-hydroxides are listed in Table 4. The intercept (A) gives the value of $\log K^0$. The standard entropy change (ΔS^0) can be calculated using the following equation:

$$\Delta S^0 = -\left(\frac{\partial \Delta G^0}{\partial T}\right)_p \quad (12)$$

The average standard enthalpy change (ΔH^0) is then calculated by using the values of ΔG^0 and ΔS^0:

$$\Delta G^0 = \Delta H^0 - T\Delta S^0 \quad (13)$$

The relative parameters obtained from the Eqs. (11)–(13) are listed in Table 4. The positive ΔH^0 values means that the holistic process of U(VI) sorption is an apparently endothermic. The possible reason to this endothermic sorption has been clarified in previous study in detail.[13,35] The negative values of ΔG^0 indicate that sorption process is spontaneous with high affinity of U(VI) to iron oxy-hydroxides. ΔG^0 becoming increasingly negative with an increase in temperature indicates that the spontaneous nature of sorption of U(VI) is directly proportional to temperature. The positive entropy change (ΔS^0) reflects the affinity of iron oxy-hydroxides toward U(VI) ions in aqueous solutions and possibly suggests that the strong sorption such as inner-sphere complexes dominate U(VI) sorption accompanied by the release of H_2O molecules from the hydration shell of U(VI).

3.7 Sorption mechanism

The SCM is employed in exploring the sorption species and mechanism of U(VI) on the iron oxy-hydroxides combined MINTEQ 3.0 and constant capacity model (CCM). The sorption species as a function of pH is shown in Fig. 8 and the relative sorption constants are list in Table 1 as well. The SCM suggested the main sorption

species of U(VI) on the iron oxy-hydroxides are $\equiv S^{s}OUO_2^{+}$ (log$K$ = 1.65) at pH <4.5, $\equiv S^{w}OUO_2OH^{0}$ (log$K$ = -8.00) and $\equiv S^{w}OUO_2(CO_3)_2^{3-}$ (log$K$ = 17.50) above pH 4.5. The three kinds of inner-sphere complexes can precisely explain the sorption edge of U(VI) under the observed pH range, which actually coincided with the discussion above. One of our previous work found that U(VI) sorption on attapulgite/iron oxide magnetic composites can be interpreted and indicated that the main sorption species were $\equiv S^{s}OUO_2^{+}$ (log$K$ = -1.78) and $\equiv S^{w}OUO_2(CO_3)_2^{3-}$ (log$K$ = 20.50).[44] These sorption species on the composites are basically consistent with this study here. Niu et al.[16] studied the mechanism of U(VI) sorption on attapulgite and found that the sorption species consist of one ion exchange species ($\equiv X_2UO_2^{0}$) at acid condition and an inner-sphere complex ($\equiv S^{w}OUO_2OH^{0}$) at high pH range.

The sorption constant (i.e., K^0) calculated from the SCM and thermodynamic is compared to give more information about the sorption mechanism. For the SCM, value of K at pH 4.5 is deduced from the following reactions:

$$\equiv Fe^{w}O^{-} + UO_2OH^{+} \leftrightarrow \equiv Fe^{w}O(UO_2OH)^{0} \qquad \log K^{0} = 5.44 \qquad (14)$$

$$\equiv Fe^{s}O^{-} + UO_2^{2+} \leftrightarrow \equiv Fe^{s}OUO_2^{+} \qquad \log K^{0} = 4.03 \qquad (15)$$

$$\equiv Fe^{w}O^{-} + UO_2(CO_3)_2^{4-} \leftrightarrow \equiv Fe^{w}O\,UO_2(CO_3)_2^{3-} \qquad \log K^{0} = 3.20 \qquad (16)$$

If mono-dentate complexes are forming for U(VI) sorption on iron oxy-hydroxides, the K^0 can be defined as the following:

$$K^{0}=Q/(C_e\cdot\Gamma) = K_d/\Gamma \qquad (17)$$

where Q (mol/g) and C_e (mol/L) are, respectively, the concentration of U(VI) in solid and aqueous phases during sorption reaches equilibrium; Γ represents the fraction of unoccupied sorption sites. According to the total sorption site capacity and the sorption amount of U(VI) on iron oxy-hydroxides at 25 °C as shown in Fig. 8, Γ is close to 1.0 in this study, therefore K^0 can be approximately equivalent to K_d. In practice, the extrapolated method of logK_d vs. C_e suggests that the apparent sorption reaction constant logK^0 is about 3.41. Basing on the contribution of each species of

U(VI) on the iron oxy-hydroxides at pH 4.5, the apparent reaction constant $\log K^0$ is about 4.08 (= 5.2% × $\log K^0$ (≡$Fe^wOUO_2OH^0$) + 94.0% × $\log K^0$ (≡$Fe^sOUO_2^+$) + 0.8% × $\log K^0$ (≡$Fe^wOUO_2(CO_3)_4^{3-}$)). The results suggested that the apparent $\log K^0$ deduced from K_d is quite close to that optimized by the SCM. This finding suggests that mono-dentate complexes are forming for U(VI) sorption on the iron oxy-hydroxides and that the extrapolated method through K_d can be used to estimate the apparent sorption constant.

Conclusions

The kinetic process of U(VI) sorption on iron oxy-hydroxides can be described well by the pseudo-second-order kinetics model and the Weber-Morris model. The intra-particle diffusion is the main rate limitation step for the sorption of U(VI) on iron oxy-hydroxides. Generally, pH can strongly affect U(VI) sorption on the iron oxy-hydroxides, whereas the large ionic strength only weakly inhibit U(VI) sorption, especially at high pH. The presence of HA could promote U(VI) sorption to iron oxy-hydroxides at acidic conditions, but restricts U(VI) sorption obviously at alkaline conditions. SCM and the batch sorption data suggested that mono-dentate inner-sphere complexes should be responsible for U(VI) sorption on the iron oxy-hydroxides. The sorption species of U(VI) under the observed pH range consists of ≡$Fe^sOUO_2^+$, ≡$Fe^wO(UO_2OH)^0$ and ≡$Fe^wOUO_2(CO_3)_2^{3-}$. These findings are crucial to evaluate the immobilization of uranium at the solid/water interface in the environment.

Acknowledge *Financial support from Special Foundation for High Level Waste Disposal, China (No. [2012] 494) and National Natural Science Foundation of China (21327801, J1210001, 21101083, 91226113) are acknowledged.*

References

1 S. Goldberg, L.J. Criscenti, D.R. Turner, J.A. Davis, K.J. Cantrell, *Vadose Zone J.* 2007, **6**, 407–435.

2 K. Müller, H. Foerstendorf, T. Meusel, V. Brendler, G. Lefèvre, M.J. Comarmond, T.E. Payne, *Geochim. Cosmochim. Acta* 2012, **76**, 191–205.

3 P. Thakur, R.C. Moore, G.R. Choppin, *Radiochim. Acta* 2005, **93**, 385–391.

4 Y. Arai, M. McBeath, J.R. Bargar, J. Joye, J.A. Davis, *Geochim. Cosmochim. Acta* 2006, **70**, 2492–2509.

5 N.K. Pandey, *Oxid. Commun.* 2006, **29**, 698–707.

6 R. Drot, J. Roques, E. Simoni, *C. R. Chim.* 2007, **10**, 1078–1091.

7 N. Jordan, C. Lomenech, N. Marmier, E. Giffaut, J.J. Ehrhardt, *J. Coll. Interf. Sci.* 2009, **329**, 17–23.

8 D. Li, D.I. Kaplan, *J. Hazard. Mater.* 2012, **243**, 1–18.

9 C.J. Dodge, A.J. Francis, J.B. Gillow, G.P. Halada, C. Eng, C.R. Clayton, *Environ. Sci. Technol.* 2002, **36**, 3504–3511.

10 S.E. Aamrani, J. Giménez, M. Rovira, F. Seco, M. Grive, J. Bruno, L. Duro, J. DePablo, *Appl. Surf. Sci.* 2007, **253**, 8794–8797.

11 M. Rovira, S.E. Aamrani, L. Duro, J. Giménez, J.D. Pablo, J. Bruno, *J. Hazard. Mater.* 2007, **147**, 726–731.

12 D.M. Singer, S.M. Chatman, E.S. Ilton, K.M. Rosso, J.F. Banfield, G.A.Waychunas, *Environ. Sci. Technol.* 2012, **46**, 3821−3830.

13 Q.H. Fan, J.Z. Xu, Z.W. Niu, P. Li, W.S. Wu, *Appl. Radiat. Isot.* 2012, **70**, 13–19.

14 P. Li, Q.H. Fan, D.Q. Pan, S.P. Liu, W.S. Wu, *J. Radioanal. Nucl. Chem.* 2011, **289**, 757–764.

15 X.L. Tan, P.P. Chang, Q.H. Fan, X. Zhou, S.M. Yu, W.S. Wu, X.K.Wang, *Coll. Surf. A* 2008, **328**, 8–14.

16 Z.W. Niu, Q.H. Fan, W.H. Wang, J.Z. Xu, L. Chen, W.S. Wu, *Appl. Radiat. Isot.* 2009, **67**, 1582–1590.

17 Z.S. Chu, W.X. Liu, H.X. Tang, T.W. Qian, S.S. Li, Z.T. Li, G.B. Wu, *J. Coll. Interf. Sci.* 2002, **252**, 426–432.

18 N. Kannan, M.M. Sundarum, *Dyes Pigments* 2001, **51**, 25–40.

19 S.L.G. Petroni, M.A.F. Pires, C.S. Munita, *J. Radioanal. Nucl. Chem.* 2004, **259**, 239–243.

20 Y.S. Ho, G.H. McKay, *Water Res.* 2000, **34**, 735–742.

21 K.G. Bhattacharyya, A. Sharma, *Dyes Pigments* 2005, **65**, 51–59.

22 M. Alkan, Ö. Demirbaş, M. Doğan, *Micropor. Mesopor. Mat.* 2007, **101**, 388–396.

23 D.B. Wu, J. Zhao, L. Zhang, Q.S. Wu, Y.H. Yang, *Hydrometallurgy* 2010, **101**, 76–83.

24 Y. Vijaya, S.R. Popuri, V.M. Boddu, A. Krishnaiah, *Carbohyd. Polym.* 2008, **72**, 261–271.

25 G. Montavon, S. Markai, Y. Andres, B. Grambow, *Environ. Sci. Technol.* 2002, **36**, 3303–3309.

26 E.R. Sylwester, E.A. Hudson, P.G. Allen, *Geochim. Cosmochim. Acta* 2000, **64**, 2431–2438.

27 T. Hattori, T. Saito, K. Ishida, A.C. Scheinost, T. Tsuneda, S. Nagasaki, S. Tanaka, *Geochim. Cosmochim. Acta* 2009, **73**, 5975–5988.

28 A. Rossberg, K.U. Ulrich, S. Weiss, S. Tsushima, T. Hiemstra, A.C. Scheinostt, *Environ. Sci. Technol.* 2009, **43**, 1400–1406.

29 K. Müller, H. Foerstendorf, V. Brendler, A. Rossberg, K. Stolze, A. Gröschel, *Chem. Geol.* 2013, **357**, 75–84.

30 T. Yamaguchi, S. Nakayama, T. Yoshida, *Radiochim. Acta* 2004, **92**, 677–682.

31 D.L. Zhao, X.B. Wang, S.T. Yang, Z.Q. Guo, G.D. Sheng, *J. Environ. Radioactiv.* 2012, **103**, 20–29.

32 X.L. Tan, Q.H. Fan, X.K. Wang, B. Grambow, *Environ. Sci. Technol.* 2009, **43**, 3115–3121.

33 C.L. Chen, D. Xu, X.L. Tan, X.K. Wang, *J. Radioanal. Nucl. Chem.* 2007, **273**, 227−233.

34 B.H. Gu, J. Schmitt, Z. Chen, L.Y. Liang, J.F. McCarthy, *Environ. Sci. Technol.* 1994, **28**, 38–46.

35 Q.H. Fan, X.L. Tan, J.X. Li, X.K. Wang, W.S. Wu, G. Montavon, *Environ. Sci. Technol.* 2009, **43**, 5776–5782.

36 S.T. Yang, D.L. Zhao, H. Zhang, S.S. Lu, L. Chen, X.J. Yu, *J. Hazard. Mater.* 2010, **183**, 632–640.

37 E. Tertre, G. Berger, E. Simoni, S. Castet, E. Giffaut, M. Loubet, H. Catalette, *Geochim. Cosmochim. Acta* 2006, **70**, 4563–4578.

38 W.S. Wu, Q.H. Fan, J.Z. Xu, Z.W. Niu, S.S. Lu, *Appl. Radiat. Isot.* 2007, **65**, 1108–1114.

39 S. Wang, Y. Boyjoo, A. Choueib, Z.H. Zhu, *Water Res.* 2005, **39**, 129–138.

40 B.B. Johnson, *Environ. Sci. Technol.* 1990, **24**, 112–118.

41 P.H. Tewari, A.B. Campbell, W. Lee, *Can. J. Chem.* 1972, **50**, 1642–1648.

42 P. Sharma, R. Tomar, *J. Coll. Interf. Sci.* 2011, **362**, 144–156.

482 43 F.E. Bartell, T.L. Thomas, Y. Fu, *J. Phys. Chem.* 1951, **55**, 1456–1462.

483 44 Q.H. Fan, P. Li, Y.F. Chen, W.S. Wu, *J. Hazard. Mater.* 2011, **192**, 1851–1859.

Tables

Table 1 Modeling parameters and sorption constants for U(VI) sorption on iron oxy-hydroxides

1. Iron oxy-hydroxides description	
Capacitance (F) = 1.75 F/m^2	
$T[\equiv Fe^wOH]^a = 8.816\times10^{-4}$ mol/g, $T[\equiv Fe^sOH]^b = 1.812\times10^{-4}$ mol/g.	
Reactions	logK^{int}
$\equiv Fe^wOH \leftrightarrow \equiv Fe^wO^- + H^+$	-7.54 (this work)
$\equiv Fe^wOH + H^+ \leftrightarrow \equiv Fe^wOH_2^+$	4.99 (this work)
$\equiv Fe^sOH \leftrightarrow \equiv Fe^sO^- + H^+$	-2.38 (this work)
$\equiv Fe^sOH + H^+ \leftrightarrow \equiv S^sOH_2^+$	3.54 (this work)
$\equiv Fe^sOH + UO_2^{2+} \leftrightarrow \equiv Fe^sOUO_2^+ + H^+$	1.65 (this work)
$\equiv Fe^wOH + UO_2^{2+} + H_2O \leftrightarrow \equiv Fe^wO(UO_2OH)^0 + 2H^+$	-8.00 (this work)
$\equiv Fe^wOH + UO_2^{2+} + 2CO_3^{2-} \leftrightarrow \equiv Fe^wO\,UO_2(CO_3)_2^{3-} + H^+$	17.50 (this work)
2. The reaction of U(VI) in aqueous solution[16,44]	
$UO_2^{2+} + H_2O \leftrightarrow UO_2OH^+ + H^+$	-5.25
$UO_2^{2+} + 2H_2O \leftrightarrow UO_2(OH)_{2(aq)} + 2H^+$	-12.15
$UO_2^{2+} + 3H_2O \leftrightarrow UO_2(OH)_3^- + 3H^+$	-20.25
$UO_2^{2+} + 4H_2O \leftrightarrow UO_2(OH)_4^{2-} + 4H^+$	-32.40
$UO_2^{2+} + CO_3^{2-} \leftrightarrow UO_2CO_{3(aq)}$	9.94
$UO_2^{2+} + 2CO_3^{2-} \leftrightarrow UO_2(CO_3)_2^{2-}$	16.61
$UO_2^{2+} + 3CO_3^{2-} \leftrightarrow UO_2(CO_3)_3^{4-}$	21.84

[a] $T[\equiv Fe^wOH] = [\equiv Fe^wOH_2^+] + [\equiv Fe^wOH] + [\equiv Fe^wO^-]$

[b] $T[\equiv Fe^sOH] = [\equiv Fe^sOH_2^+] + [\equiv Fe^sOH] + [\equiv Fe^sO^-]$

Table 2 Simulation of kinetic data using different models.

Model	Equation (linearization)	Parameters	*R*	Ref.
pseudo-first-order model	$\frac{1}{q_t}=\frac{k_1}{q_e}\times\frac{1}{t}+\frac{1}{q_e}$	K_1=8.3190 (min^{-1}) q_e=5.8858 (mg/g)	0.9148	Kannan and Sundarum[18]
pseudo-second-order model	$\frac{t}{q_t}=\frac{1}{k_2q_e^2}+\frac{t}{q_e}$	K_2=0.0046 ($g\cdot mg^{-1}\cdot min^{-1}$) q_e=6.6845 (mg/g)	0.9997	Petroni et al.[19]
Weber-Morris model	$q_t=K_{int}t^{\frac{1}{2}}+C$	K_{int1}=0.3284 ($mg\cdot min^{1/2}\cdot g^{-1}$) C_1=2.4529 (mg/g) K_{int2}=0.0966 ($mg\cdot min^{1/2}\cdot g^{-1}$) C_2=4.0266 (mg/g) K_{int3}=0.0037 ($mg\cdot min^{1/2}\cdot g^{-1}$) C_3=6.1453 (mg/g)	0.9994 0.9686 0.9929	Alkan et al.[22]

Table 3 The parameters of the Langmuir and Freundlich models

I	Langmuir model			Freundlich model		
T (K)	q_{max} (mol/g)	b (L/mol)	R	K_F ($mol^{1-n} \cdot L^n/g$)	n	R
298 K	8.4097×10^{-5}	6.7524×10^{4}	0.9964	0.0036	0.4171	0.9822
318 K	1.6965×10^{-4}	2.1403×10^{4}	0.9958	0.1240	0.7410	0.9809
338 K	2.1452×10^{-4}	2.4241×10^{4}	0.9943	0.1159	0.7007	0.9833

Table 4 The linear fit of logK_d vs. C_e (logK_d = A+B·C_e) and thermodynamic parameters for U(VI) sorption on the iron oxy-hydroxides

T (K)	logK_d = A+B·C_e			Thermodynamic data		
	A	B	R	ΔG^0 (kJ/mol)	ΔH^0(kJ/mol)	ΔS^0(J /(mol·K))
298.15	3.4123	-5115.8090	0.9876	-19.47	11.61	
318.15	3.4753	-4048.3112	0.9858	-21.17	11.99	104.25
338.15	3.6532	-4750.6040	0.9887	-23.64	11.62	

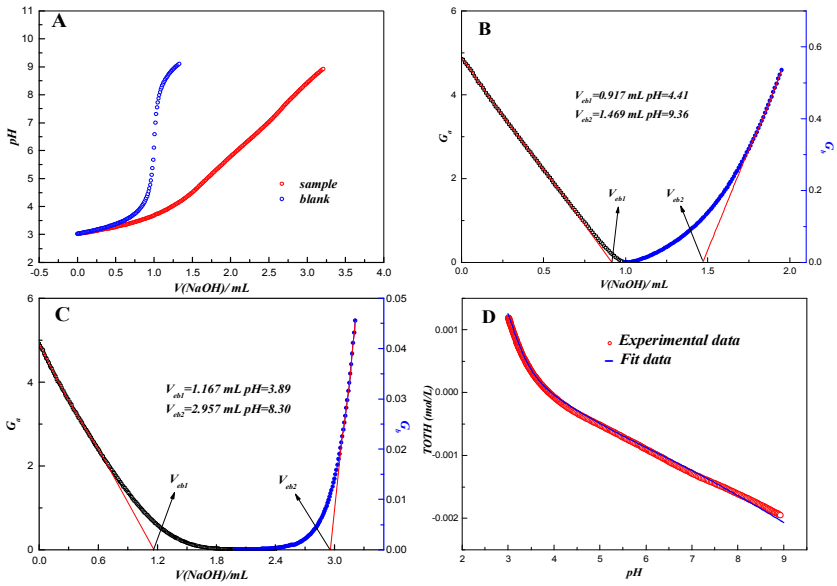

Fig. 1. (A) Titration curves of iron oxy-hydroxides and blank; (B) The Gran plots of the back-titration data of blank; (C) The Gran plots of the back-titration data of the iron oxy-hydroxides; (D) Model description and actual acid–base titration of iron oxy-hydroxides. *s/l* = 5.0 g/L, *I* = 0.01 mol/L $NaClO_4$, *T* = 25±1 ^{0}C.

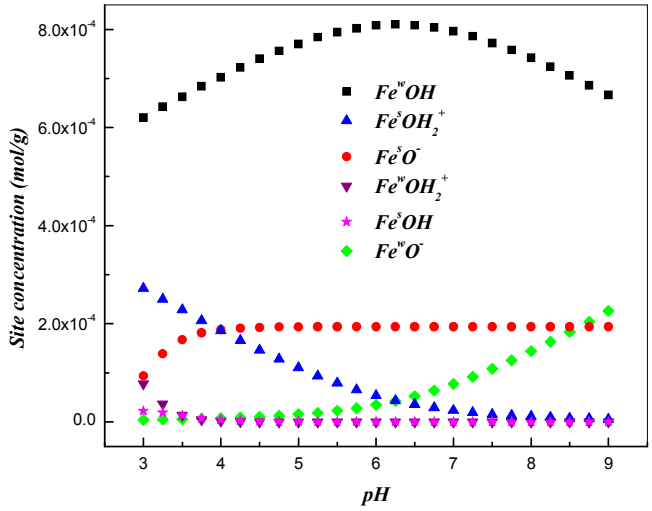

Fig. 2. Site distribution of iron oxy-hydroxides as function of pH values in 0.01 mol/L $NaClO_4$ solution. *s/l* = 5.0 g/L; *T* = 25±1 ^{0}C.

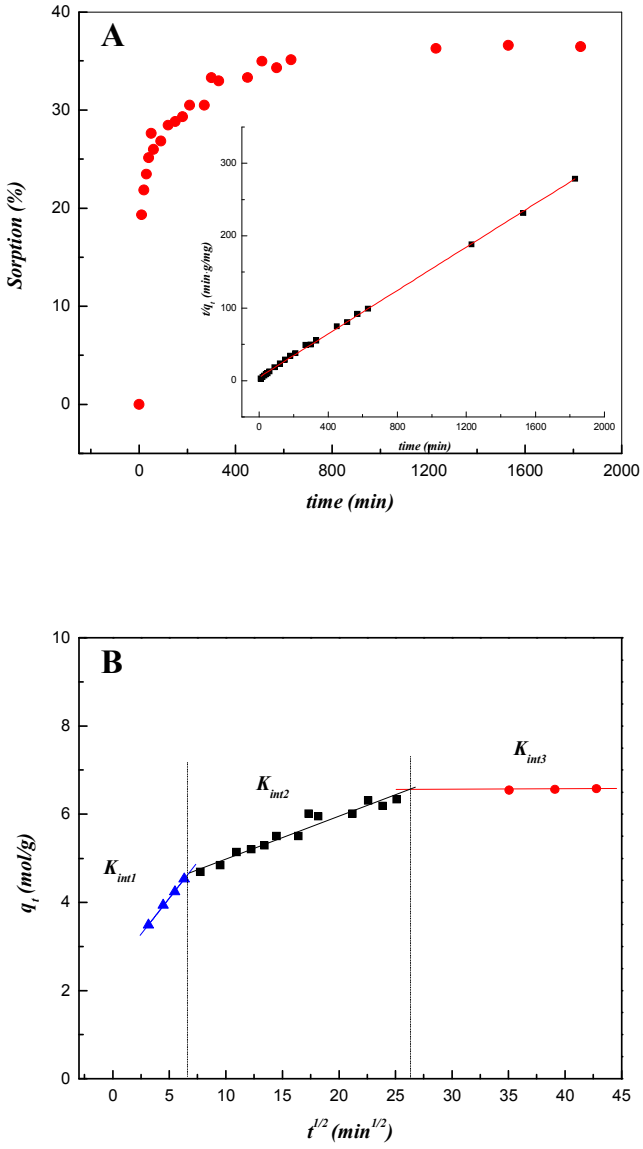

Fig. 3. (A) Effect of contact time on U(VI) sorption on iron oxy-hydroxides. *s/l* = 0.3 g/L; *I* = 0.01 mol/L $NaClO_4$; $C(UO_2^{2+})$ = 2.0×10^{-5} mol/L; *pH* = 4.5; *T* = 25±1 ^{0}C. (B) Weber-Morris kinetic equation for sorption of U(VI) on iron oxy-hydroxides.

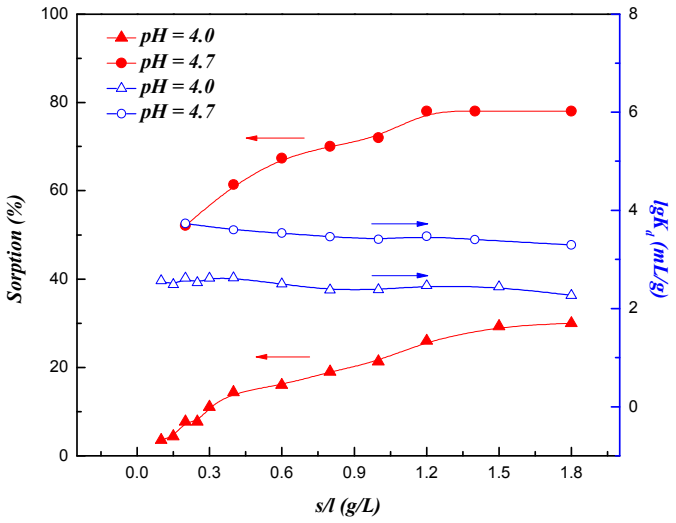

Fig. 4. Effect of solid-to-liquid (*s/l*) ratio on U(VI) sorption. C(UO_2^{2+}) = 2.0×10^{-5} mol/L; I = 0.01 mol/L $NaClO_4$; T = 25±1 ^{0}C.

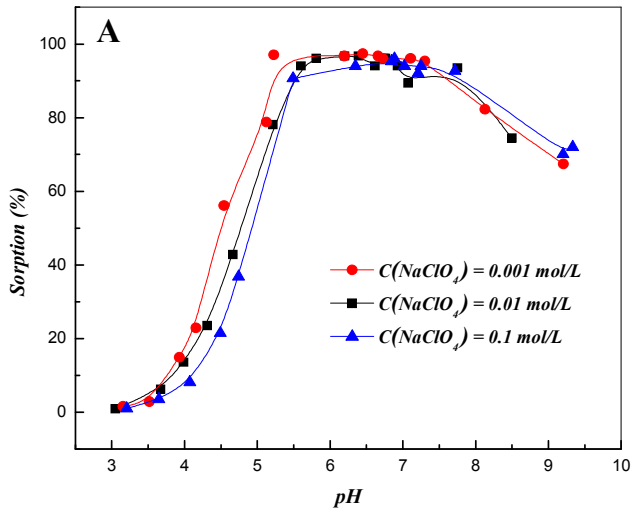

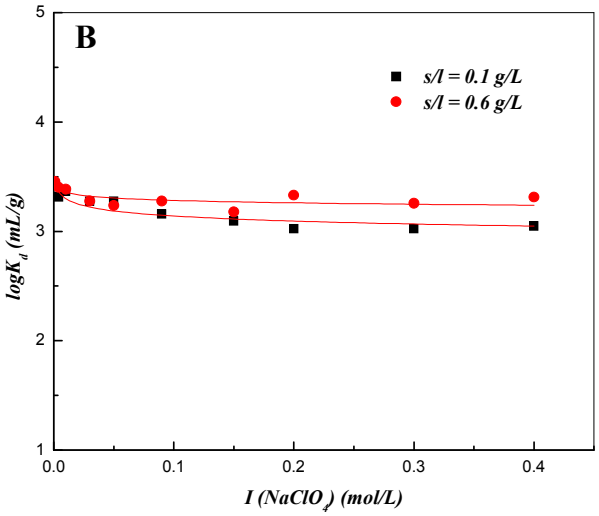

Fig. 5. (A) Effect of pH and ionic strength on U(VI) sorption onto iron oxy-hydroxides. *s/l* = 0.3 g/L; $C(UO_2^{2+}) = 2.0\times10^{-5}$ mol/L; $T = 25\pm1\ ^0C$. (B) Effect of ionic strength on U(VI) sorption. *s/l* = 0.3 g/L; $C(UO_2^{2+}) = 2.0\times10^{-5}$ mol/L; pH = 4.0±0.05; $T = 25\pm1\ ^0C$.

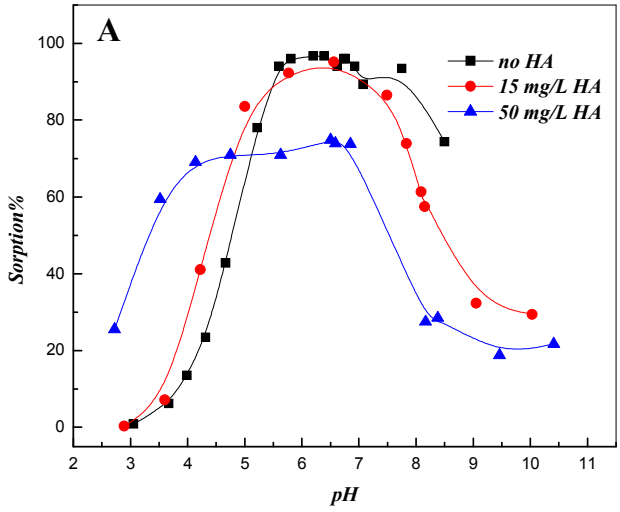

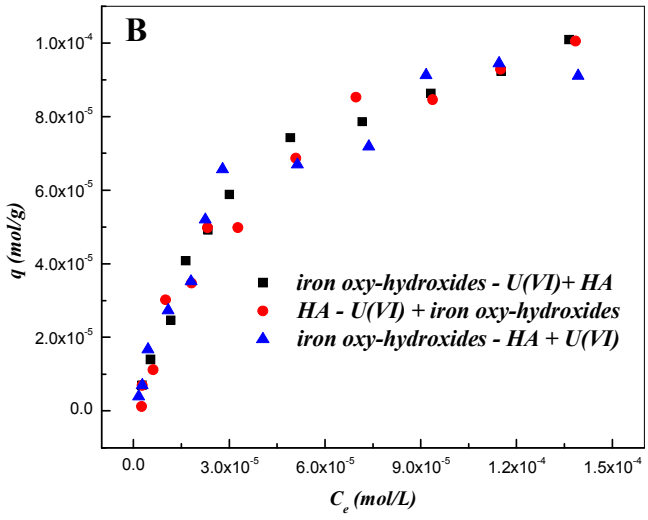

Fig. 6. (A) Effect of HA on the sorption of U(VI) as a function of pH; (B) Influence of the addition sequence of the ternary iron oxy-hydroxides/HA/U(VI) systems. ■: iron oxy-hydroxides and U(VI) were firstly equilibrated prior to the addition of HA (Iron oxy-hydroxides-U(VI) + HA), ●: U(VI) and HA were firstly equilibrated prior to the addition of iron oxy-hydroxides (HA-U(VI) + iron xoy-hydroxides), ▲: iron oxy-hydroxides and HA were firstly added prior to the addition of U(VI) (Iron oxy-hydroxides-HA + U(VI)). *s/l* = 0.3 g/L; C(HA) = 20 mg/L; *I* = 0.01 mol/L $NaClO_4$; *pH* = 4.5; *T* = 25±1 ^{0}C.

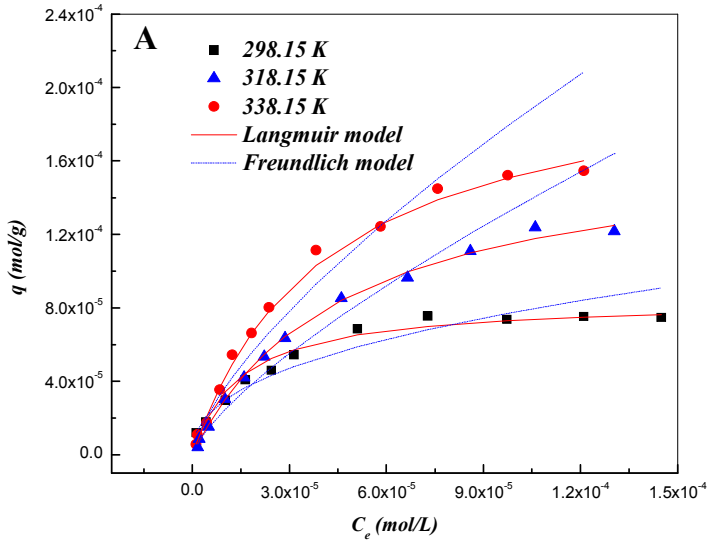

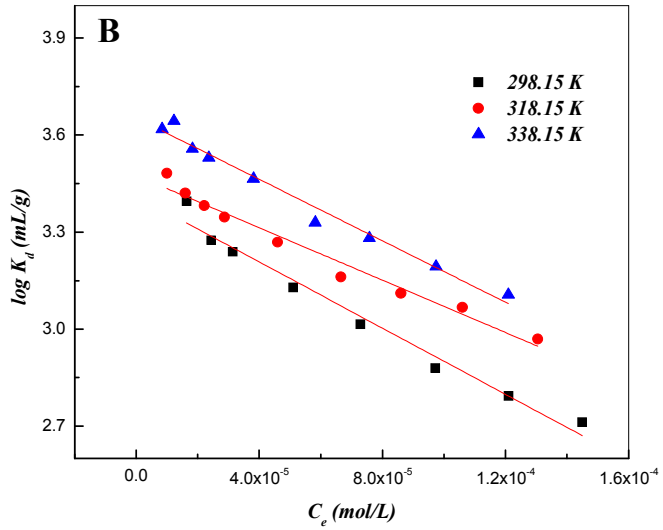

Fig. 7. (A) Sorption isotherm of U(VI) on iron oxy-hydroxides at different temperatures. s/*l* = 0.3 g/L; *I* = 0.01 mol/L $NaClO_4$; *pH* = 4.5; *T* = 25±1 ^{0}C. (B) Linear fit of logK_d vs. C_e using isotherms of U(VI) sorption on iron oxy-hydroxides. *s/l* = 0.3 g/L; *I* = 0.01 mol/L $NaClO_4$; *pH* = 4.5; *T* = 25±1 ^{0}C.

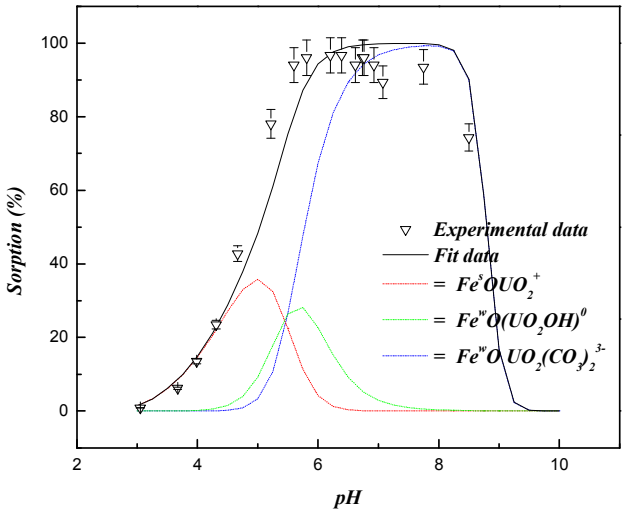

Fig. 8. The sorption species of U(VI) on iron oxy-hydroxides as a function of pH. *s/l* = 0.3 g/L; *I* = 0.01 mol/L $NaClO_4$; *T* = 25±1 ^{0}C; C(UO_2^{2+}) = 2.0×10^{-5} mol/L.